Lasers in Surgery and Medicine 26:76–82 (2000)

Preliminary Evaluation of Two Fluorescence Imaging Methods for the Detection and the Delineation of Basal Cell Carcinomas of the Skin

Stefan Andersson-Engels , PhD,[1] Gianfranco Canti, MD,[2] Rinaldo Cubeddu, PhD,[3]* Charlotta Eker, MSc,[1] Claes af Klinteberg, PhD,[1] Antonio Pifferi, PhD,[3] Katarina Svanberg, PhD, MD,[4] Sune Svanberg, PhD, MDhc,[1] Paola Taroni, PhD,[3] Gianluca Valentini, PhD,[3] and Ingrid Wang, PhD, MD[4]

[1]Lund University Medical Laser Centre, Department of Physics, SE-22100 Lund, Sweden
[2]University of Milan, Department of Pharmacology, I-20129 Milan, Italy
[3]INFM, Politecnico di Milano, Department of Physics and CEQSE-CNR, I-20133 Milan, Italy
[4]Department of Oncology, Lund University Hospital, SE-221 85 Lund, Sweden

Background and Objective: **Fluorescence techniques can provide powerful noninvasive means for medical diagnosis, based on the detection of either endogenous or exogenous fluorophores. The fluorescence of δ-aminolevulinic acid (ALA)-induced protoporphyrin IX (PpIX) has already shown promise for the diagnosis of tumors. The aim of the study was to investigate the localization of skin tumors after the topical application of ALA, by detecting the PpIX fluorescence either in the spectral or in the time domain.**
Study Design/Materials and Methods: **Two fluorescence imaging systems were used to identify basal cell carcinomas of the skin in humans, after topical application of 20% ALA ointment. Both systems rely on the comparison between the exogenous and the endogenous fluorescence, performed either in the spectral domain or in the time domain. The first system works by using three images acquired through different spectral filters, whereas the second one measures the spatial map of the average fluorescence lifetime of the sample.**
Results: **A clear demarcation of skin malignancies was successfully performed in vivo noninvasively with both fluorescence imaging systems.**
Conclusion: **The two complementary approaches considered in the present study show promise for skin tumor detection and delineation based on specific fluorescence features. Lasers Surg. Med. 26:76–82, 2000.**

Key words: basal cell carcinoma; δ-aminolevulinic acid; fluorescence imaging; protoporphyrin IX; tumor detection

INTRODUCTION

Fluorescence imaging techniques are under development for medical tissue characterization, in particular for cancer detection. Techniques based on either endogenous or exogenous fluorophores are being considered. In the latter case, effective selectivity criteria between malignant and surrounding healthy tissues have been found both in the spectral and in the time domains [1–3].

Some exogenous substances, selectively concentrating in diseased areas, are characterized by

Contract grant sponsor: European Community Access to Large Scale Facilities Programme; Contract grant number: ERBFMGECT950020.

*Correspondence to: Rinaldo Cubeddu, PhD, Dipartimento di Fisica, Politecnico di Milano, Piazza Leonardo da Vinci 32, I-20133 Milan, Italy.
E-mail: rinaldo.cubeddu@fisi.polimi.it

Accepted 4 October 1999

distinctive spectral fluorescence features. Hence, by subtracting and/or dividing two or more images acquired in different wavelength regions from tissue containing such a drug, an artificial image can, with a suitable matrix algorithm, be formed to provide an optimal contrast for malignant lesions [4].

In the time domain approach, pulsed excitation and time-delayed detection can result in a successful identification of diseased areas, usually relying on the longer lifetime of exogenous dyes such as porphyrins, compared with the natural fluorescence [5,6]. A system capable of calculating a lifetime image, i.e., the spatial distribution of the fluorescence decay time, can exploit such behavior for diagnostic purposes [7].

Various exogenous dyes have been extensively studied for demarcating malignant lesions and for their photosensitizing capability, which is of interest for photodynamic therapy (PDT). Most of these studies have been performed with systemically administered drugs. An appealing alternative to the intravenous injection is the topical administration of δ-aminolevulinic acid (ALA), a photoinactive precursor of the naturally occurring protoporphyrin IX (PpIX). As most photosensitizing agents useful for PDT, PpIX is also strongly fluorescent. The fluorescence contrast has been shown to be good enough to allow the clear demarcation of pathologic areas, thus suggesting the possible use of ALA/PpIX for tumor detection [8]. The topical administration of ALA is feasible for skin lesions [8,9], instillation for bladder tumors [10], and inhalation for pathologies of the bronchi [11,12]. Topical use avoids systemic side effects such as skin photosensitization, which may be a concern for clinical use.

In the present study, the spectroscopic characterization of basal cell carcinomas (BCC) of the skin after topical application of ALA was carried out. Two different imaging systems were used, working in the spectral and in the time domains, respectively. The main aims of the study were to assess the capacity of the two imaging modalities to identify BCC and to determine whether the two approaches can provide complementary information, to increase the potential of fluorescence imaging for tumor detection. The present study describes preliminary clinical results obtained in patients affected by BCC.

MATERIALS AND METHODS

Patients

Two patients (called B and P in this study) were included in the study. Patient B was an 81-year-old man with two nodular BCC located on the trunk (25 × 15 mm and 20 × 10 mm, respectively). The other patient (P), a 39-year-old man, had three lesions of nevoid basal cell carcinoma syndrome (Gorlin syndrome). These lesions all had a diameter of approximately 10 mm, and were all located on the trunk.

Experimental Procedure

The ALA ointment was freshly prepared by mixing 20% (w/w) ALA (Porphyrin Products, Utah) with an oil-in-water emulsion (Essex cream). The ointment was topically applied onto the lesions and a 1-cm margin of surrounding skin at time $t = 0$. An occlusive bandage was put on the lesions. Two hours later, the ALA ointment was carefully removed and the fluorescence measurements were carried out. The ointment and the bandage was then reapplied and the fluorescence measurements were repeated at $t = 3$ hours.

Before acquiring the images, fluorescence spectra were recorded inside and outside the lesion area, by using a point-monitoring fluorosensor. Thereafter, normal photographs, multicolor, and lifetime images of each lesion were recorded in sequence. The investigation was performed at Lund University Hospital, with approval from the local ethics committee.

Fluorescence Spectroscopy

Laser-induced fluorescence spectra were recorded between 450 and 730 nm, by using a point-monitoring fluorosensor described in detail elsewhere [13]. Briefly, a nitrogen laser-pumped dye laser tuned to 405 nm was used for excitation, and an optical multichannel analyzer (OMA) was used for detection. A 600-μm core diameter optical fiber, with the distal end placed in light contact with the skin, allowed both delivery of the excitation light and collection of the fluorescence signal. Point measurements were performed in the center of and 4 mm outside each lesion. Spectra were not corrected for the response of the OMA sensor.

Multicolor Imaging

Multicolor imaging was carried out by simultaneously recording three spatially identical, but spectrally different images with the same inten-

sified CCD video camera, by using a system developed for endoscopic applications [4,14]. The images were spectrally separated in three wavelength bands by means of dichroic mirrors. One (named A) was in the red region (580–750 nm), one (B) in the blue region (420–480 nm), and one (D) in the green-yellow region (480–580 nm). The fluorescence was induced by means of pulsed ultraviolet light (390 nm) from a frequency-doubled alexandrite laser. The excitation light was delivered by an optical fiber, and the fluorescence light was collected through a laryngoscope. The gated image intensifier was synchronized with the laser. A gate width of 500 ns was used to efficiently suppress the ambient room light. Thereby, a normal reflected light image could be recorded simultaneously by using a color CCD video camera. Recorded fluorescence images were digitized in a frame grabber and stored on a PC/486 computer. Calculations were subsequently carried out on the digitized images. The function:

$$F_c = (A - k_1 D)/k_2 B \tag{1}$$

with A, B, and D defined above, and k_1 and k_2 being constants with different values for different applications, was used to produce images with optimized contrast between the lesions and adjacent normal tissue. The PC computed the F_c value pixel by pixel and fed the result, by means of an output frame grabber, to a video mixer, where the fluorescence image could be mixed with the normal image from the color CCD camera.

Lifetime Imaging

The basic elements of the lifetime imaging system were a nitrogen laser-pumped dye laser, emitting 1-ns pulses at 405 nm, and an intensified CCD video camera. The intensifier could be gated with a rise time of 2 ns. An orange cut-off filter (Kodak Wratten no. 22) was used to remove the scattered laser light and to reduce the natural fluorescence background. The images were acquired and processed by high performance image boards installed in a PC/486 computer [7].

In the present study, five gated images were recorded from each lesion by using the delays: 0, 3, 5, 10, and 20 ns, with respect to the excitation pulses. Overall, the acquisition procedure took less than 3 seconds. Then, the images were processed according to the algorithm briefly outlined in the following.

Based on a simplified model, the fluorescence intensity $I(t)$ can be assumed to be a mono-exponential function of time. Image acquisition corresponds to time integration and spatial sampling, which lead to the following matrix representation of the irradiance $H(d_k)$, as a function of the acquisition delay d_k

$$\begin{aligned} H(d_k) &= C \int_{d_k}^{\infty} I(t)dt \\ &= C\tau I(0)\exp(-d_k/\tau), \quad (k = 1..5) \end{aligned} \tag{2}$$

where τ is the decay time matrix, and C is a constant, depending on the system set-up. The excitation pulse defines the time origin $t = 0$.

With simple algebra, the spatial distribution of the decay time τ can be obtained from a linear regression involving the five delayed images or only some of them. Thereafter, the amplitude matrix $A = \mathrm{I}(0)$ can also be calculated. Both matrices can be plotted in gray shade or pseudocolor images.

RESULTS

The fluorescence spectra acquired from the center of the lesions (e.g., Fig. 1a) are always dominated by the typical emission line shape of PpIX, with a main peak at 635 nm and a secondary maximum around 700 nm. On the other hand, a few millimeters outside the lesions, the PpIX fluorescence is very weak or not detected at all and the collected signal, which is due to the natural fluorescence, peaks in the blue-green region of the spectrum (e.g., Fig. 1b). The intensity of the natural emission is always significantly weaker in the tumor than in the adjacent normal tissue, whereas the line shapes are very similar.

Figure 2 shows a photograph of a region containing the lesion, the spectrum of which is depicted in Figure 1a. The small dark area on the right is a benign nevus, whereas the reddish spot on the left side is the BCC.

The multicolor image of the same lesion is shown in Figure 3. The brighter the image, the higher the ratio between exogenous and endogenous fluorescence, according to the function F_c defined previously. The BCC is clearly identified, being much brighter than the surrounding tissue. Moreover, the margins of the lesion are sharply defined.

Working in the time domain to calculate the fluorescence lifetime and amplitude maps of the lesions, we repeated the linear regression three times per sample, by using the five delayed images or only some of them placed either in the

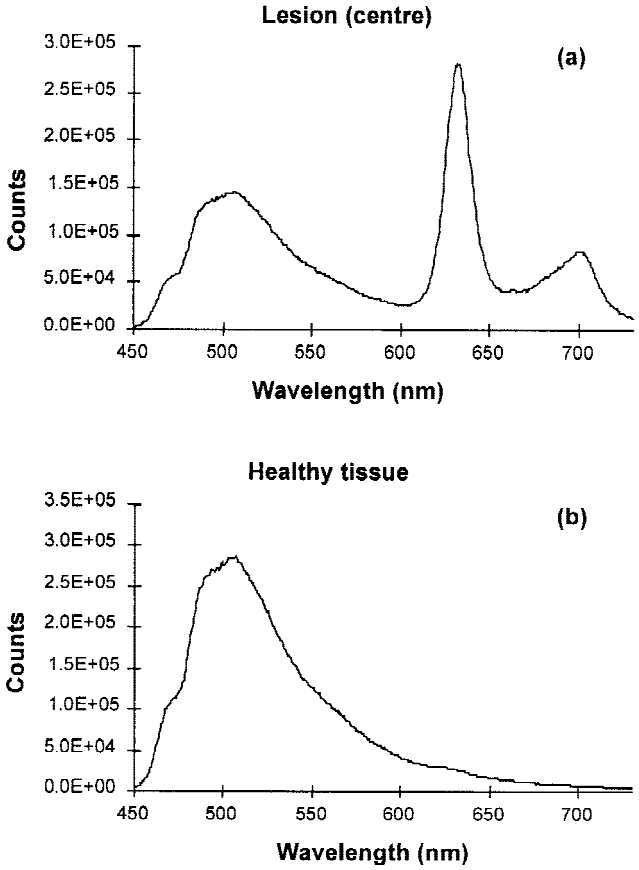

Fig. 1. Fluorescence spectra acquired 2 hours after the application of δ-aminolevulinic acid from the center (**a**) and 4 mm outside (**b**) of lesion 2 of patient P.

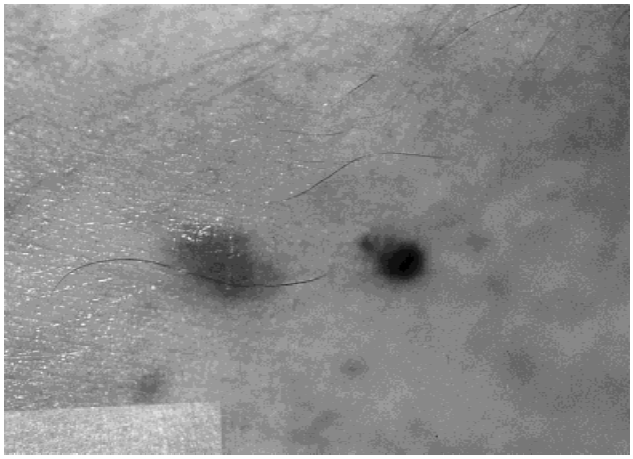

Fig. 2. Photograph of lesion 2 of patient P, the spectra of which are depicted in Figure 1.

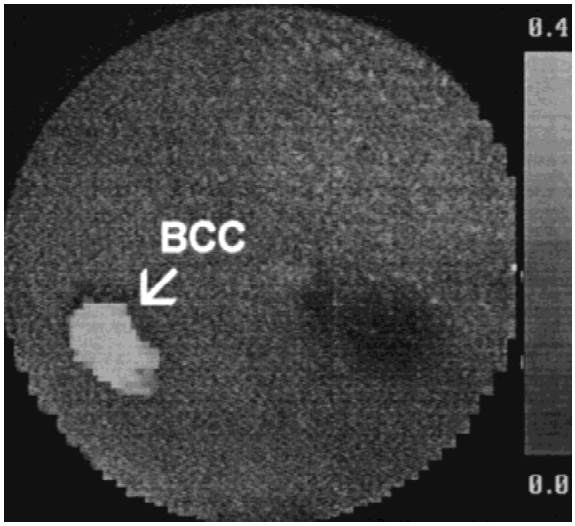

Fig. 3. Multicolor fluorescence image of the lesion shown in Figure 2. BCC, basal cell carcinoma.

short or in the long delay range. The best contrast between tumor and healthy tissue was always found by using the short-delay (0, 3, 5 ns) images for the lifetime calculation and the long-delay (10, 20 ns) images for the amplitude calculation, whereas the whole set of images gave somewhat intermediate results. Figure 4 displays the lifetime (a) and the amplitude (b) maps of the same lesion as in Figure 3. In both the amplitude and the lifetime maps, the area where the ALA cream was applied appears slightly brighter than the background. The BCC is the central spot characterized by a longer lifetime in Figure 4a and by a higher amplitude in Figure 4b. The extension of the spot coincides with the lesion as delineated by the multicolor imaging system. For the five lesions considered in this preliminary study, there was a very good agreement between the tumor areas localized by expert visual examination and those revealed by the two imaging methods. No significant differences were observed between measurements performed 2 and 3 hours after ALA application.

To obtain quantitative data from the time-resolved images, we evaluated the average amplitude and lifetime in the tumor ($\overline{A_T}$ and $\overline{\tau_T}$, respectively) and in the surrounding healthy tissue ($\overline{A_H}$, $\overline{\tau_H}$). Then, we calculated the ratios $R_A = \overline{A_T}/\overline{A_H}$ and $R_\tau = \overline{\tau_T}/\overline{\tau_H}$ to define two indices of the delineation capability of the technique. Table 1 shows the contrast ratios R_A and R_τ calculated according to the above-described criteria for best contrast, for the different lesions of the two patients. The average contrast is 1.8 (SD = 0.3) in the amplitude domain, whereas it is 1.5 (SD = 0.3) for the lifetimes.

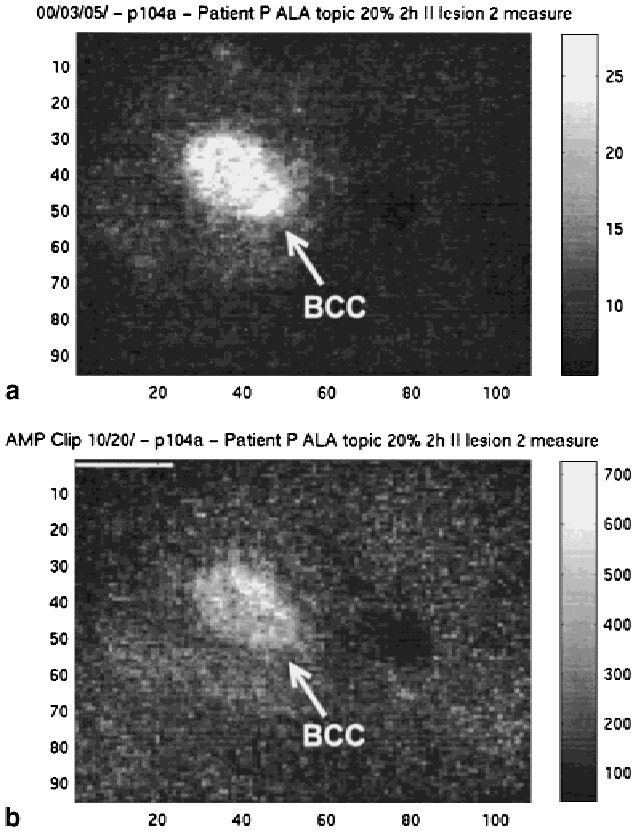

Fig. 4. Fluorescence lifetime image (**a**) and fluorescence amplitude image (**b**) of the lesion in Figures 2 and 3.

TABLE 1. Ratios of the Average Lifetime (R_τ) and Amplitude (R_A) in the Tumor and in the Surrounding Healthy Tissue 2 Hours after Application of δ-Aminolevulinic Acid

Patient	Lesion	R_τ	R_A
B	1	1.3	1.7
B	2	1.2	2.3
P	1	1.5	2.0
P	2	2.0	1.8
P	3	1.4	1.4

DISCUSSION

The multicolor approach takes advantage of two concurrent circumstances: the reduction in natural fluorescence that has been frequently observed in tumors and premalignant lesions [15], and the strong PpIX emission usually originating from neoplastic tissues after the topical application of ALA. An effective discrimination between the two fluorescence signals could be achieved in the spectral domain, because they peak at different wavelengths, as shown in Figure 1. The first image of the multicolor system gets primarily the red emission of PpIX, the second one gets the yellow-green natural fluorescence, which constitutes a background noise in the previous image, whereas the third image contains mainly the natural fluorescence at its peak. The function F_c defined in Eq. (1) leads to a dimensionless ratio between the background-free exogenous emission and the natural fluorescence. Therefore, according to the assumption above, F_c has its maximum in the tumor and allows a clear delineation of the lesion when its value is greater by a factor of 5 or more with respect to the healthy area nearby, as it is the case for the multispectral image shown in Figure 3. Being a ratio between fluorescence intensities collected in different spectral ranges, F_c is insensitive to the morphology of the illuminated area and to the possibly uneven distribution of the excitation light.

In a similar way, the average decay time of the fluorescence signal is very sensitive to the balance of the exogenous versus natural emission in tumors and in healthy tissues, because the two signals are known to differ in decay time as well as in spectral shape. In fact, the PpIX emission is long-living ($\tau > 15$ ns) [5,16], whereas the natural fluorescence of the tissue vanishes with a time constant of 5–6 ns or shorter [5]. Moreover, the biochemical alterations caused by the tumor growth often influence the decay time of exogenous fluorophores. This proved to be the case when hematoporphyrin derivative (HpD) was administered to animals bearing experimental malignant tumors [17]. A significant lengthening of the fluorescence lifetime was observed in neoplastic tissues, even when the natural fluorescence was completely removed by using a cut-off filter and long delay gates. Therefore, it was concluded that the HpD lifetime "senses" the tumor environment. Until now, this effect was demonstrated only in mice and it is more likely to be specific of HpD, being a mixture of monomers, dimers, and oligomers, whose equilibrium between different forms of aggregation might be easily affected. Nevertheless, also in the case of the PpIX, the lifetime might be influenced by the environment. This could contribute to make the lifetime in the tumor longer than in healthy tissues. Whichever effect is predominant, either the different ratio between the short-living fluorescence (natural) and the long-living one (PpIX) or the change in decay time of the drug emission due to the different environment, the net result is an average lifetime longer in the malignant tumor than in

healthy tissues. As a rule of thumb, a skin lesion can be suspected to be neoplastic when its fluorescence lifetime is longer by a factor of 1.2 or more with respect to the healthy area nearby. Also a sharp outline of the lesion borders is a strong indication of its neoplastic character. To better exploit the different contribution of the exogenous signal versus the endogenous one, the linear regression leading to the lifetime map has to be performed in the short-delay range (0–5 ns), when the natural fluorescence is still present. On the other hand, if the drug concentration has to be evaluated, the amplitude map calculated in the long-delay range is the choice. In fact, the 10 ns, or even better the 20 ns, delayed images are expected to be dominated by the PpIX fluorescence. The higher fluorescence amplitude in the tumor area shown in Figure 4b confirms that the production of PpIX is well localized in the BCC, as indicated also by the multicolor image. As a matter of fact, both approaches (amplitude and lifetime, shown in Fig. 4a,b) work in this preliminary experiment performed with a rather high sensitizer dose (ALA 20%). Nevertheless, from an extensive study on experimental tumors in mice sensitized with HpD, the authors observed that the lifetime approach still works at very low doses, when the amplitude images fail to reveal the neoplastic lesions [17]. If confirmed with ALA, this finding is a significant point in favor of the lifetime approach. Moreover, the lifetime map, being based on a dimensionless ratio, benefits from the same advantages as the multicolor contrast function F_c in terms of insensitivity to nonuniform excitation.

In this preliminary study, the performances of the two systems turned out to be similar: the five lesions were identified with the same degree of reliability. The complexity of the experimental set-ups is reasonably equivalent: the multispectral system requires custom optics for image separation, whereas the lifetime system needs a high-speed image intensifier and nontrivial synchronization electronic. As an additional drawback, the lifetime apparatus requires pulsed excitation and detection, whereas this regimen is only a nice feature for the multispectral system.

Actually, the two devices work on the basis of the same changes in exogenous and endogenous fluorescence that take place in cancerous tissue with respect to healthy ones. Therefore, a similar tumor detection and delineation capability is expected from both systems, provided that the instrumental setups are sensitive enough to fully exploit the intrinsic contrast ascribed to the biophysical effects. This is certainly true at high ALA dose, as was the case in this study. A really challenging test would require an ALA dose much lower than the one used for PDT. Then, the performances of the systems in terms of signal to noise ratio would be crucial for a reliable behavior. In such harsh conditions, a combination of the two techniques might be beneficial to improve either the sensitivity or the specificity in demarcating the tumor tissue. This result could be achieved at a reasonable cost, because the two systems share several components.

Even though the lesions considered in the present study were rather large and identifiable by visual inspection, the multispectral and lifetime techniques are expected to be applicable also for the detection of small lesions and, at least in some cases, for the localization of lesions not obviously recognizable. These potential applications, together with the accurate delineation of observable lesions, would hopefully be the long-term outcome of this research. Actually, we do not see any limitation in either instruments that could prevent the detection of skin tumors smaller than a certain dimension. The spatial resolution required to resolve small lesions can be easily achieved with a suitable optical system such as a macro lens, whereas the biochemical machinery that leads to the transformation of ALA in PpIX has been demonstrated to work also in a single cell [18].

The question of whether not-obviously-visible lesions can be detected by fluorescence imaging deserves some comments. It is rather unlikely for a patient to undergo dermatological examination without any visible sign onto the skin. Therefore, a blind search for a malignant lesion in an apparently healthy subject is really not the case. Nevertheless, patients affected by previously detected skin cancers might be profitably examined by means of this technique to discover other early lesions, nonclinically visible, possibly present on the subject. Other patients affected by a severe alteration of the skin (actinic or seborrheic dermatitis) in a large body area might be searched for cancerous lesions. In that case, the whole affected part (e.g., the face) appears reddish and deseased and it is very difficult to distinguish a malignant lesion from the underlying dermatitis. Then, fluorescence imaging could be beneficial to address punch biopsies in selected sites. To this regard, the authors had the chance to examine an elder patient affected by a serious actinic derma-

titis on his face caused by a prolonged (years) exposure to the solar radiation in a tropical country. A squamous cell carcinoma, really nondistinguishable by visual inspection, was detected thanks to the fluorescence measurements. This clinical case has not been included in this study, which focuses on BCC; nevertheless, it seems to indicate that not obviously visible lesions can be revealed by fluorescence imaging. Moreover, even when the neoplasia has been assessed by expert examination or histopathology, fluorescence imaging is very interesting to delineate the borders of the cancerous tissue, which might extend beyond the visible lesion.

In summary, both the multicolor and the lifetime imaging systems allowed a reliable demarcation of BCC, after topical ALA sensitization in the two patients considered in the present study. Further work is in progress to confirm the results obtained so far and to extend the study to a higher number of patients and to different lesion types, both benign and malignant.

REFERENCES

1. Andersson-Engels S, Berg R, Johansson J, Stenram U, Svanberg K, Svanberg S. Laser spectroscopy in medical diagnostics. In: Dougherty TJ, Henderson BW, editors. Photodynamic therapy: basic principles and clinical applications. New York: Marcel Dekker; 1992. p 387–424.
2. Cubeddu R, Taroni P, Valentini G, Canti G. Use of time-gated fluorescence imaging for diagnosis in biomedicine. J Photochem Photobiol B Biol 1992;12:109–113.
3. Andersson-Engels S, af Klinteberg C, Svanberg K, Svanberg S. In vivo fluorescence imaging for tissue diagnostics. Phys Med Biol 1997;42:815–824.
4. Svanberg K, Wang I, Colleen S, Idvall I, Ingvar C, Rydell R, Jocham D, Diddens H, Bown S, Gregory G, Montán S, Andersson-Engels S, Svanberg S. Clinical multi-colour fluorescence imaging of malignant tumours: initial experience. Acta Radiol 1998;38:2–9.
5. Andersson-Engels S, Johansson J, Svanberg S. The use of time-resolved fluorescence for diagnosis of atherosclerotic plaque and malignant tumours. Spectrochim Acta Part A Mol Spectrosc 1990;46:1203–1210.
6. Cubeddu R, Canti G, Taroni P, Valentini G. Time-gated fluorescence imaging for the diagnosis of tumors in a murine model. Photochem Photobiol 1993;57:480–485.
7. Cubeddu R, Pifferi A, Taroni P, Valentini G, Canti G. Tumor detection in mice by measurement of fluorescence decay time matrices. Opt Lett 1995;20:2553–2555.
8. Kennedy JC, Pottier RH, Pross DC. Photodynamic therapy with endogenous Protoporphyrin IX: Basic principles and present clinical experience. J Photochem Photobiol B Biol 1990;6:143–148.
9. Svanberg K, Andersson T, Killander D, Wang I, Stenram U, Andersson-Engels S, Berg R, Johansson J, Svanberg S. Photodynamic therapy of non-melanoma malignant tumours of the skin using topical δ-amino levulinic acid sensitization and laser irradiation. Br J Dermatol 1994; 130:743–751.
10. Kriegmair M, Baumgartner R, Knuechel R, Steinbach P, Ehsan A, Lumper W, Hofstädter F, Hofstetter A. Fluorescence photodetection of neoplastic urothelial lesions following intravesical instillation of 5-aminolevulinic acid. Urology 1994;44:836–841.
11. Huber RM, Gamarra F, Leberig A, Stepp H, Rick K, Baumgartner R. Inhaled 5-aminolevulinic acid (ALA) for photodynamic diagnosis and early detection of bronchial tumors: first experience in patients. Abstract book of the 6th IPA Meeting, Melbourne, Australia: March 10–14, 1996.
12. Baumgartner R, Huber RM, Schulz H, Stepp H, Rick K, Gamarra F, Leberig A, Roth C. Inhalation of 5-aminolevulinic acid: a new technique for fluorescence detection of early stage lung cancer. J Photochem Photobiol B Biol 1996;36:169–174.
13. Andersson-Engels S, Elner Å, Johansson J, Karlsson S-E, Salford L G, Strömblad L-G, Svanberg K, Svanberg S. Clinical recording of laser-induced fluorescence spectra for evaluation of tumour demarcation feasibility in selected clinical specialties. Lasers Med Sci 1991;6:415–424.
14. Andersson-Engels S, Johansson J, Svanberg S. Medical diagnostic system based on simultaneous multispectral fluorescence imaging. Appl Opt 1994;34:8022–8029.
15. Andersson-Engels S, Johansson J, Svanberg K, Svanberg S. Fluorescence imaging and point measurements of tissue: applications to the demarcation of malignant tumors and atherosclerotic lesions from normal tissue. Photochem Photobiol 1991;53:807–814.
16. Schneckenburger H, König K, Kunzi-Rapp K, Westphal-Frösch C, Rück A. Time-resolved in vivo fluorescence of photosensitizing porphyrins. J Photochem Photobiol B Biol 1993;21:143–147.
17. Cubeddu R, Canti G, Pifferi A, Taroni P, Valentini G. Fluorescence lifetime imaging of experimental tumors in hematoporphyrin derivative-sensitized mice. Photochem Photobiol 1997;66:229–236.
18. Malik Z, Dishi M, Garini Y, Fourier transform multipixel spectroscopy and spectral imaging of protoporphyrin in single melanoma cells. Photochem Photobiol 1996;63: 608–614.